JOURNAL OF MATERIALS SCIENCE 26 (1991) 4026–4032

Effect of niobium additions on the structure and magnetic properties of equiatomic iron–cobalt alloys

A. I. C. PERSIANO*, R. D. RAWLINGS
Department of Materials, Imperial College of Science, Technology and Medicine, London SW7 2BP, UK

The structure of equiatomic iron–cobalt alloys containing 1, 2 and 3 wt% niobium has been studied using a variety of techniques, including X-ray diffraction, scanning and transmission electron microscopy and differential thermal analysis. It has been found that niobium is effective in reducing the kinetics of ordering to the B2 structure and of anti-phase domain growth, even though the solubility is only 0.3–0.5 wt%. The magnetic properties (coercive force and saturation magnetization) and the electrical resistivity of the three alloys have also been determined.

1. Introduction

Equiatomic FeCo-base alloys are well-established soft magnetic alloys which are particularly noted for their high saturation magnetization. Commercially available alloys contain small quantities of a ternary addition in order to facilitate fabrication at room temperature. The most commonly employed addition is vanadium, and typically about 2 wt % is added. The role of vanadium is through its effect on the transformation from the high-temperature disordered b.c.c. structure to the low-temperature ordered B2 structure, which commences at 730 °C in the binary alloy. It is established that vanadium permits the ductile b.c.c. structure to be more readily retained by quenching to room temperature, or lower, from above the order–disorder transformation temperature [1, 2], even though vanadium has a negligible effect on the ordering kinetics when a metastable disordered sample is isothermally heat-treated at temperatures below 600 °C. The transformation to the brittle, ordered state is so rapid in the binary equiatomic alloy that it is impossible, under industrial conditions, to retain the more malleable, disordered structure. During production of the ternary alloy, the material is quenched into cold brine from the hot-rolling temperature, which is above the order–disorder transformation temperature, so enabling the final cold fabrication to be carried out with the alloy in the b.c.c. condition.

Although the vanadium-containing alloy may be obtained in the metastable, disordered state by quenching, the quenching conditions are critical and it would be desirable if they could be relaxed. It is for this reason that Rawlings and co-workers [1–3, 7, 8, 10], in cooperation with Telcon Metals Ltd, have been investigating the effects of different ternary additions on the order–disorder transformation and the properties of Fe–Co alloys. This paper reports the results of a study of the effects of niobium additions of 3 wt % and less. It is, of course, paramount that any ternary addition should not degrade the good soft magnetic properties of the binary equiatomic alloy, and consequently magnetization and coercive measurements have been made. The electrical resistivity was also determined.

2. Experimental procedure

Ingots of three FeCo–Nb alloys, with equiatomic proportions of Fe and Co, were prepared by arc-melting the constituent elements under an argon atmosphere. Each ingot weighed approximately 50 g and the niobium contents were 1, 2 and 3 wt %. The ingots were ground, hot-rolled, quenched to retain disorder and finally cold-rolled about 75% to a thickness of 0.25 mm.

Differential thermal analysis (DTA) was performed on hot-rolled samples in order to determine the order–disorder and α–γ transition temperatures.

The cold-rolled alloys were heat-treated for 2 h under flowing argon at 850 °C, followed by either (i) quenching into iced brine to produce the metastable, disordered state, or (ii) furnace-cooling to allow time for the fully ordered state to develop. The alloys in these two starting conditions were then subjected to isochronal heat-treatments of 1 h at temperatures in the range 500 to 750 °C and isothermal heat-treatments at 550 °C for times of 1 to 32 h.

At various stages in the heat-treatments, the structure of the alloys was determined by means of light microscopy, scanning and transmission electron microscopy and X-ray diffraction (CoK_α radiation). The latter technique was used to obtain the degree of

* *Present address*: Departamento de Fisica-UFMG, CP 702, 30161 Belo Horizonte-MG, Brazil.

0022–2461/91 $03.00 + .12

long-range order, S, from the intensities of the superlattice {1 0 0} peak and the fundamental {2 0 0} peak. These peaks were chosen since the textures in the alloys [2, 3] would affect both peaks in a similar manner. A previous neutron diffraction study of FeCo–2% V [4] showed the maximum degree of long-range order to be 0.8, so the present results were normalized to this value for the fully ordered condition. In addition to monitoring changes in S, X-ray diffraction was used to calculate the size of the anti-phase domain (APD) boundaries from the associated broadening, b, of the superlattice peaks according to

$$D = \frac{K\lambda}{b\cos\theta} \quad (1)$$

where K is a constant, λ the wavelength and θ the diffraction angle. In order to account for contributions to the broadening from sources other than the domains, b was determined from measurements of the half-breadths of the {1 0 0} superlattice peak (B) and the {2 0 0} fundamental peak (B') using

$$b^2 = B^2 - B'^2 \quad (2)$$

Lattice parameters were also determined by X-ray diffraction using CuK_α radiation.

The magnetic properties were assessed using a ballistic method for ring specimens in accordance with British Standards [5]. Rings of 25 mm outer diameter and 20 mm inner diameter were spark-eroded from 0.25 mm strip and stacked to give a ring specimen approximately 1 mm thick. The maximum field applied to saturate the specimens was 4000 A m^{-1}. Measurements were made on the alloys in the furnace-cooled condition.

The electrical resistivity of the alloys in the ordered and disordered conditions was determined at − 196 °C using the four-point method. The geometry of the specimens (nominal dimensions were 40 mm × 1 mm × 0.25 mm) and the placement of the contacts minimized the errors involved in using the following equation for resistivity, ρ, rather than more cumbersome expressions [6]

$$\rho = RA/l \quad (3)$$

where R is the resistance, A the cross-sectional area and l the distance between the voltage contacts.

For comparison purposes some experiments were carried out on a commercial FeCo–2% V alloy and two equiatomic alloys containing 3.6 and 5.4 wt % V, which were produced by the same procedures as the FeCoNb alloys.

The typical experimental errors of the measurements mentioned in this section are displayed as error-bars in most of the figures referred to in the next section.

3. Results

The DTA results for the vanadium and niobium alloys are presented in Fig. 1. The lower-temperature peak, which showed negligible hysteresis on heating and cooling, corresponds to the order–disorder transition and the other peak is due to the α–γ transformation.

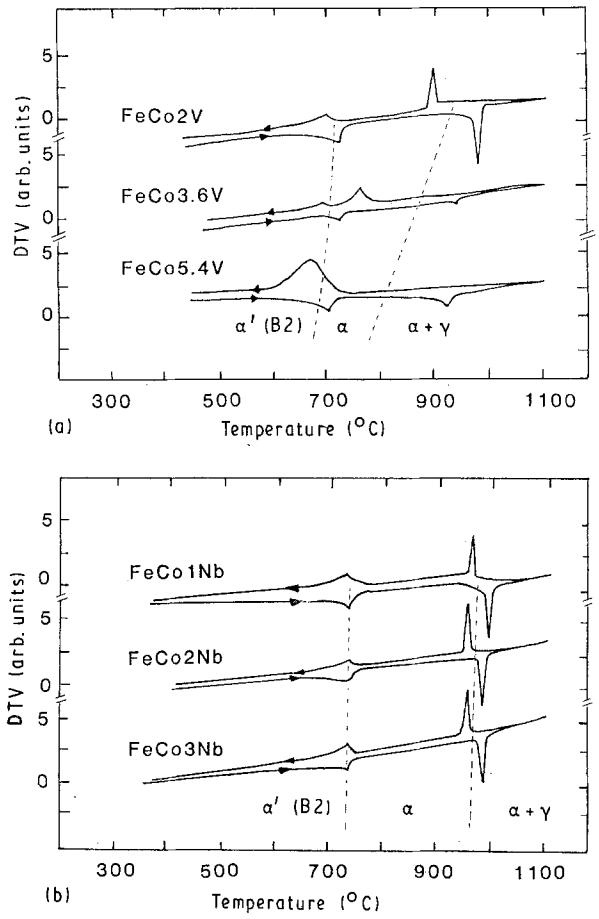

Figure 1 Differential thermal voltage (DTV) as a function of temperature for (a) equiatomic FeCo–V alloys and (b) equiatomic FeCo–Nb alloys. The heating/cooling rate was 5 °C min^{-1}.

The locus of the mean of the peak temperatures on heating and cooling is given by the dotted lines in Fig. 1. It can be seen that the order–disorder transition temperature, T_c, for the niobium alloys was effectively constant at 731 ± 2 °C, which is in agreement with the value of 730 °C usually quoted for the equiatomic binary alloy. In contrast the transition temperatures were lower for the vanadium-containing alloys, e.g. 713 °C for the FeCo–2% V alloy, and fell with increasing vanadium content. The characteristics of the α–γ transformation temperatures were similar in that the temperatures were higher for the niobium-containing alloys and were not so dependent on the amount of addition.

The niobium-containing alloys in both the quenched and furnace-cooled conditions contained a second phase, the proportion of which increased with increasing niobium content (Fig. 2 and Table I). A Mössbauer spectroscopy study by the authors [7, 8] also demonstrated that the volume fraction of the second phase increased with niobium content as well as showing that the second phase was paramagnetic. The second phase was mainly in the form of fine, spherical particles (Fig. 3) although there were colonies consisting of the second phase in a slightly less spherical morphology. These colonies are the large pale areas on the scanning electron micrographs of Fig. 2. Energy-dispersive analysis of the spherical particles in a thin foil showed them to be rich in niobium, their average composition being 49 at % Co,

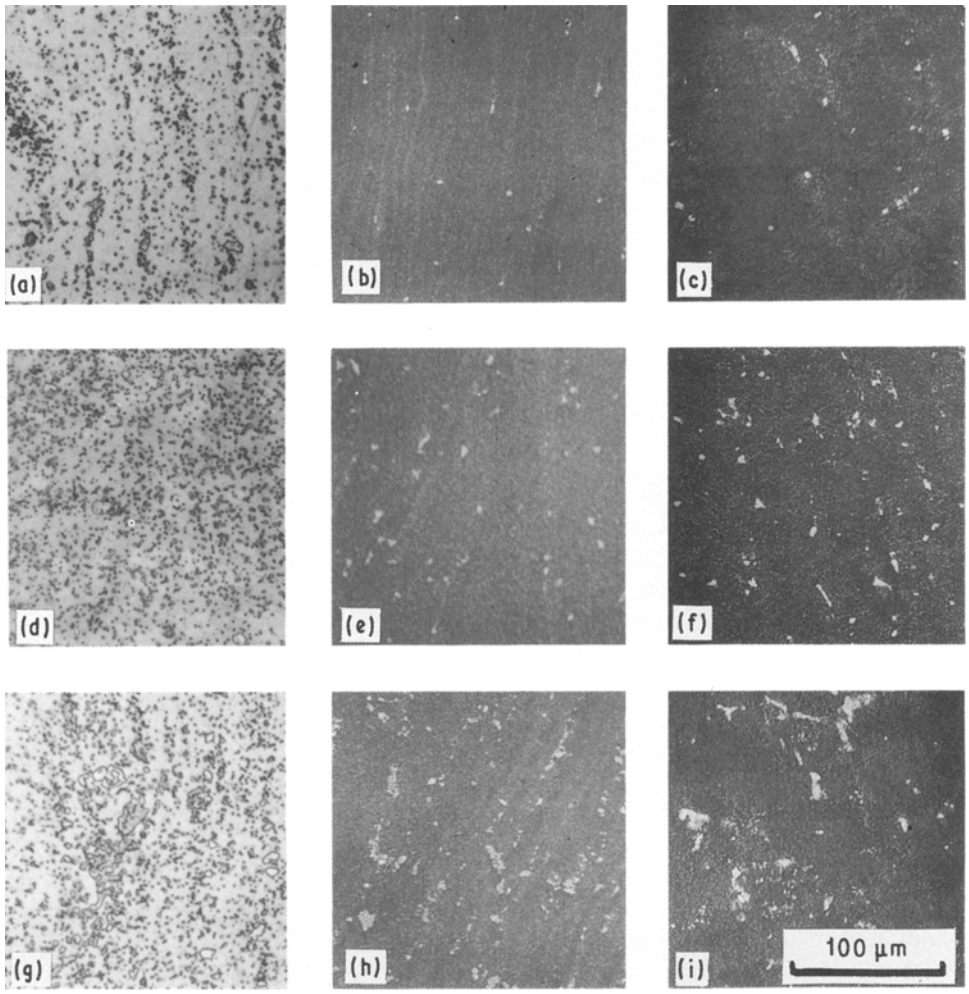

Figure 2 Micrographs showing γ_2 precipitates in FeCo–Nb alloys: (a, b, c) FeCo–1% Nb; (d, e, f) FeCo–2% Nb; (g, h, i) FeCo–3% Nb. (a, b, d, e, g, h) Quenched; (c, f, i) furnace-cooled; (a), (d) and (g) are light micrographs and the others back-scattered electron micrographs.

TABLE I Grain size (d) and proportion (p) of second phase in FeCo–Nb alloys in furnace-cooled and quenched conditions

Nb content (wt %)	Furnace-cooled		Quenched	
	d (μm)	p (%)	d (μm)	p (%)
1	41	7	33	6
2	20	11	18	10
3	15	14	15	11

35 at % Fe and 16 at % Nb. In this sense the particles are similar to the $L1_2\gamma_2$ phase reported in FeCo alloys with vanadium and vanadium plus nickel additions, which have been found to be rich in vanadium and nickel [9, 10]. The second phase will be referred to as γ_2 in the following text because of the similarities with the γ_2 phase in FeCoV alloys, i.e. paramagnetic and rich in ternary addition, even though the $L1_2$ structure has not been confirmed. The grain size of the matrix, as measured by the linear intercept method, was smaller the greater the amount of niobium, and hence proportion of γ_2 in the alloy (Table I).

The effect of isochronal heat-treatment on the degree of long-range order of FeCo–1% Nb in the furnace-cooled (curve A, ordered) and quenched (curve B, disordered) conditions is shown in Fig. 4.

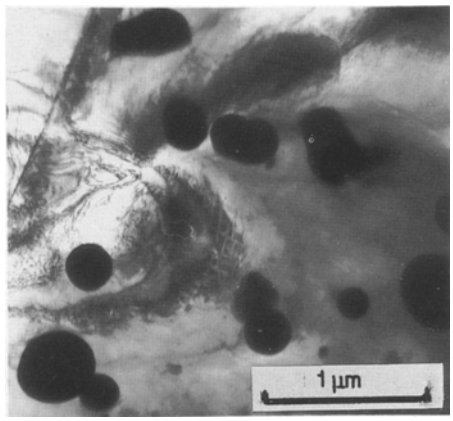

Figure 3 Transmission electron micrograph of the γ_2 particles in FeCo–1% Nb alloy quenched and heat-treated for 1 h at 630 °C.

Curve A exhibits a continuous decrease in S with increasing temperature, extrapolating to $S = 0$ at the transition temperature T_c of 731 ± 2 °C. On the other hand, curve B for the initially disordered material has a positive slope up to about 690 °C. Between 690 °C and T_c the two curves coincide, indicating that it is not until these high temperatures that the equilibrium degree of long-range order is achieved within 1 h for both furnace-cooled and quenched starting conditions of the alloy.

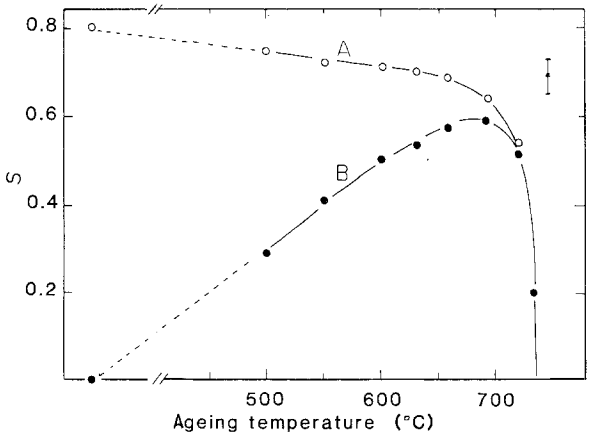

Figure 4 Long-range order parameter (S) of FeCo–1% Nb as a function of heat-treatment temperature (heat-treatment time, 1 h): alloy initially in (○) ordered and (●) disordered condition.

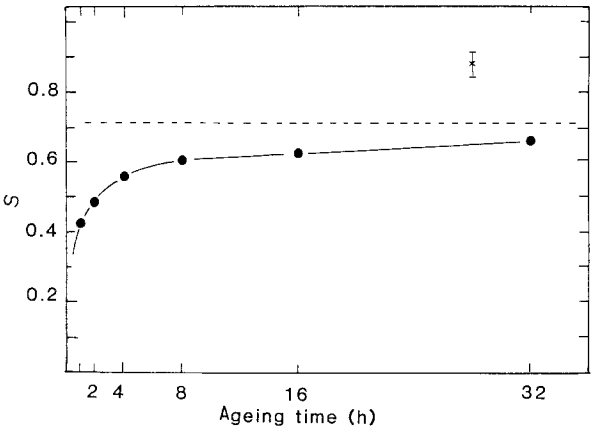

Figure 5 Long-range order parameter (S) of FeCo–1% Nb, initially in the disordered condition, as a function of heat treatment time at 550 °C. The broken line gives the equilibrium value of S at this temperature.

Isothermal heat treatment of the initially disordered, quenched material produced an asymptotic increase in S to the equilibrium value at 550 °C of about 0.7 (Fig. 5). It is interesting to note that this equilibrium value was not reached within the maximum time of 32 h used in the investigation.

The changes in the lattice parameter, a_0, after isochronal heat-treatment of the FeCo–1% Nb alloy at temperatures below the transition temperature, T_c, are presented in Fig. 6. It has been reported that a_0 for ordered equiatomic FeCo-base alloys is greater than that of the alloys in the disordered state [1, 11]. Thus, by comparison with Fig. 4, it may be concluded that the increase in a_0 on heat-treating the quenched alloy at 500 and 550 °C is due to ordering, and that the decrease in a_0 at temperatures in excess of 660 °C for both the quenched and furnace-cooled material is due to the reduction in S as T_c is approached. An additional process, such as precipitation, must be occurring over the temperature range 575 to 660 °C to account for the decrease in a_0 which takes place at lower temperatures than those required to give a significant reduction in S.

The lattice parameter of the quenched alloy as a function of time of heat-treatment at 550 °C is shown

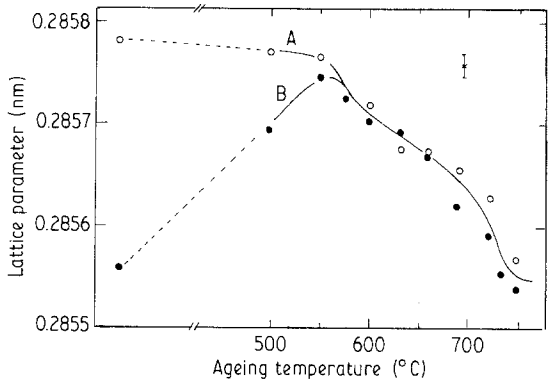

Figure 6 Lattice parameter (a_0) of FeCo–1% Nb as a function of heat-treatment temperature (heat-treatment time, 1 h): alloy initially in (○) ordered and (●) disordered condition.

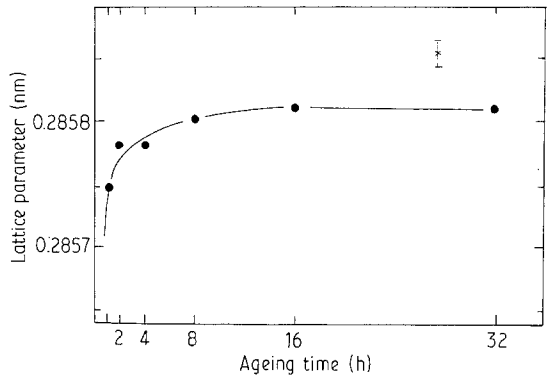

Figure 7 Lattice parameter (a_0) of FeCo–1% Nb, initially in the disordered condition, as a function of heat-treatment time at 550 °C.

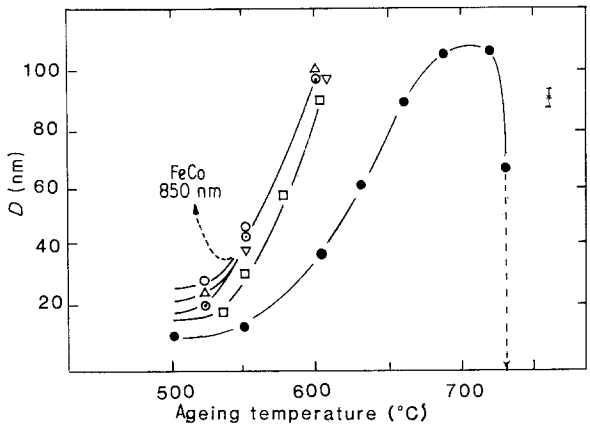

Figure 8 Antiphase domain size (D) as a function of heat-treatment temperature (heat-treatment time, 1 h) for various equiatomic alloys: (▽) FeCo, (○) FeCo–0.71% V, (△) FeCo–1.64% V and (⊙) FeCo–2.45% V [11], (□) FeCo–2% V [12] and (●) FeCo–1% Nb (present work).

in Fig. 7. The curve of Fig. 7 is of identical form to the S versus time plot of Fig. 5.

The heat-treatment temperature and time, t, dependences of the APD size, D, are presented in Figs 8 and 9, respectively. D increased with increasing temperature until T_c was approached, at which point the APD size rapidly fell. As far as the time dependence is concerned, a $t^{1/2}$ relationship was observed as previously reported in equiatomic FeCo–V [11, 12].

The electrical resistivity of the niobium- and vanadium-containing alloys in the furnace-cooled and

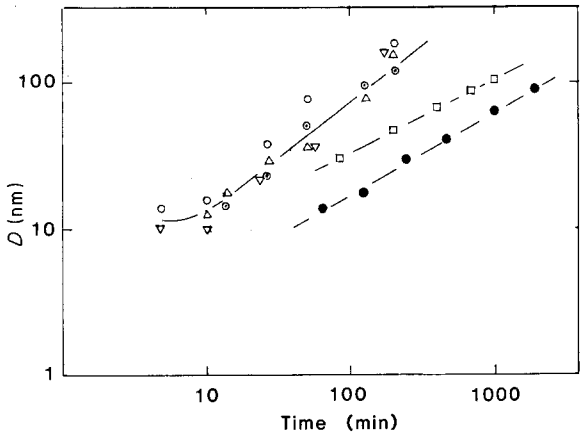

Figure 9 Antiphase domain size (D) as a function of time of heat treatment at 550 °C for various equiatomic alloys: (▽) FeCo, (○) FeCo–0.71% V, (△) FeCo–1.64% V and (⊙) FeCo–2.45% V [11], (□) FeCo–2% V [12] (●) and FeCo–1% Nb (present work).

TABLE II Electrical resistivity at −196 °C of FeCo-base alloys in furnace-cooled (FC) and quenched (Q) conditions

Alloy	Resistivity (μΩ cm)	
	FC	Q
FeCo [13]	1.95	3.09
FeCo2V	46.4	41.9
FeCo3.6V	48.2	47.5
FeCo5.4V	48.4	60.7
FeCo1Nb	3.13	5.07
FeCo2Nb	3.06	5.27
FeCo3Nb	3.16	5.50

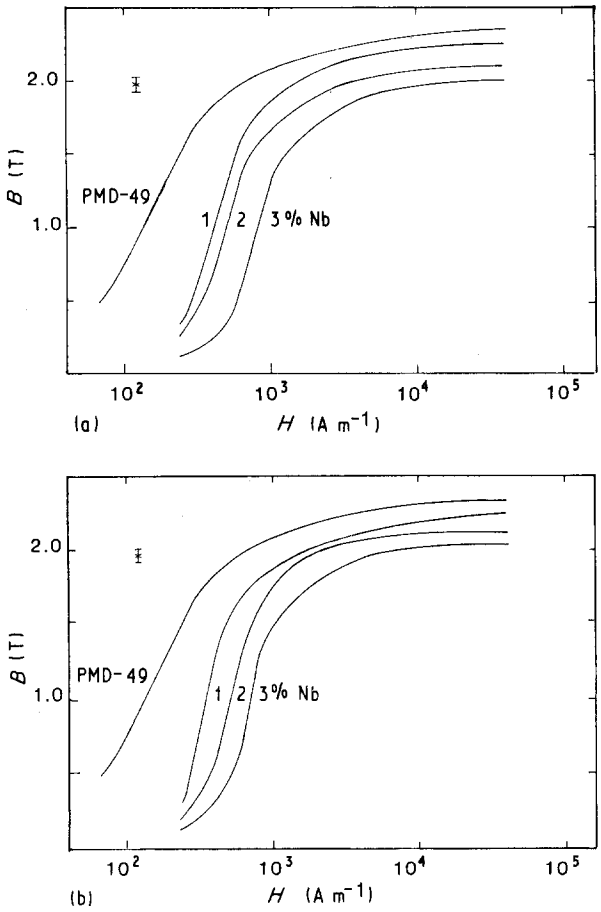

Figure 10 Magnetization curves for FeCo–Nb and FeCo–2% V (Telcon Supermendur 49) alloys, furnace-cooled from (a) 760 °C and (b) 850 °C.

quenched conditions is compared with the results due to Rossiter [13] for an equiatomic binary alloy in Table II. The resistivity of the FeCo–Nb alloys and the binary alloy was less in the ordered (furnace-cooled) state than in the disordered state, whereas the reverse was found for the two lower vanadium-content alloys. However, the most noticeable feature of the data is the much greater resistivities of the FeCo–V alloys.

Magnetization curves for the commercial FeCo–2% V alloy (Telcon Supermendur 49: PMD-49) and the FeCo–Nb alloys, furnace-cooled from 760 and 850 °C, are given in Fig. 10. The coercive force increased and the saturation magnetization decreased with increasing niobium content, and the soft magnetic properties were inferior to the FeCo–2% V alloy (Table III). The magnetization curves obtained for the higher vanadium-content alloys were displaced to higher fields and lower magnetizations than the curve for the FeCo–3% Nb alloy.

TABLE III Coercive force (H_c) and saturation magnetization (B_s) of FeCo-base alloys furnace-cooled from various temperatures

Alloy	FC from 760 °C		FC from 850 °C	
	H_c (A m^{-1})	B_s (T)	H_c (A m^{-1})	B_s (T)
FeCo1Nb	355	2.34	300	2.32
FeCo2Nb	470	2.29	425	2.24
FeCo3Nb	665	2.2	610	2.12
FeCo2V	95	2.32	90	2.35
FeCo3.6V	990	2.01		
FeCo5.4V	3930[a]	1.66[a]		

[a] FC from 550 °C.

4. Discussion

4.1. Structural observations

The presence of a niobium-rich second phase, termed γ_2, demonstrates that the solubility limit for niobium in equiatomic FeCo has been exceeded. This is supported by the DTA data, which showed only minor changes in the order–disorder and α–γ transformation temperatures with niobium content in the range 1 to 3 wt % (Fig. 1). Furthermore, the similarity of these temperatures with the corresponding temperatures for the binary alloy indicates that niobium solubility is limited. This was confirmed by the energy-dispersive analysis of the matrix, which was not able to quantify the niobium peak above the background noise, and is consistent with the conclusion drawn from an earlier Mössbauer spectroscopy investigation that the solubility limit is 0.3 to 0.5 wt % Nb [8].

The data of Table I suggest that the proportion of γ_2 is slightly greater in the furnace-cooled condition; this could be interpreted as a consequence of further precipitation occurring during the furnace-cooling from 850 °C. This evidence alone is not sufficient to

prove that further precipitation has taken place, as the changes in the volume percentage of γ_2 are small and within experimental error. However, the anomalous changes in the lattice parameter in the temperature range 575 to 660 °C for both the quenched and furnace-cooled samples (Fig. 6) are also consistent with niobium being removed from the matrix by precipitation. On the other hand, it may be concluded from the absence of any anomalous behaviour in the change in a_0 on heat-treating the quenched FeCo–1% Nb alloy at temperatures up to 550 °C, and from the similarity between the plots of S and a_0 versus time, that there is no precipitation at these temperatures.

The decrease in grain size as the niobium content of the alloy is raised is undoubtedly associated with the concomitant increase in the volume percentage of the second phase. That the presence of γ_2 reduces the grain size in FeCo-base alloys has been demonstrated by Pitt and Rawlings [10] using a variety of vanadium- and nickel-containing alloys, and this was attributed mainly to the restriction of primary grain growth by the second-phase particles. However, the grain size for a given volume percentage of γ_2 was considerably greater in the FeCo–Nb alloys than in the alloys previously investigated. It is therefore suggested that solute atoms are also playing a role in determining primary grain growth. A consequence of the more limited solubility of niobium compared to vanadium and nickel would be the observed larger grain sizes for the FeCo–Nb alloys.

The ease with which the FeCo–Nb alloys could be cold-rolled after quenching indicated that niobium retarded the transformation to the brittle ordered state. This was confirmed by the isochronal and isothermal heat-treatment experiments, which showed that the ordering kinetics in the FeCo–1% Nb alloy are relatively slow. This is clearly illustrated in Fig. 11, where the ordering behaviour on heat-treating the quenched alloy at 550 °C is compared with similar data available in the literature.

As well as slowing down the rate of ordering, niobium reduces the APD growth rate compared with the binary and vanadium-containing alloys (Figs 8 and 9). The expression for the temperature, T, and time, t, dependence of the APD size, D, is [12]

$$D^2 - D_0^2 = Kt\exp(-Q/RT) \quad (4)$$

where D_0 is the apparent value of D at $t = 0$, K is a constant and Q is the activation energy of APD growth. The latter was calculated to be 232 kJ mol^{-1} in the temperature range 550–660 °C, which is similar to the value of 255 kJ mol^{-1} reported for FeCo–2% V [12]. It follows that the smaller APD sizes for the FeCo–Nb alloy is not a result of a marked change in the activation energy but must be due to differences in the constant K.

4.2. Properties

The electrical resistivity of the FeCo–Nb alloys is significantly less than that of the FeCo–V alloys. This is in part due to the smaller amount of niobium in solution, but not solely. From the data for the furnace-cooled FeCo, FeCo–2% V and FeCo–1% Nb alloys the resistivity per atomic per cent ternary addition in solution, assuming all the vanadium and 0.3 at % Nb are in solution, is calculated to be 20.2 and 3.9 μΩ cm per atomic per cent for vanadium and niobium, respectively. Thus vanadium in solution is about five times as effective in increasing the resistivity of equiatomic FeCo as niobium. The furnace-cooled condition was chosen for this calculation as this is the condition of FeCo-based soft magnetic materials in service. The same general conclusion as to the relative effectiveness of the two ternary additions may be drawn from the results for the quenched alloys, but with the factor reduced from five to about three. The effects of niobium, and other ternary additions, on the resistivity of ordered and disordered FeCo alloys are discussed in more detail elsewhere [14].

A decrease in B_s with increasing volume percentage of second phase is observed for both FeCo–V and FeCo–Nb alloys (Fig. 12). This is a consequence of the presence of the paramagnetic γ_2 phase reducing the proportion of the ferromagnetic material that can be saturated, i.e. a dilution effect which has been reported

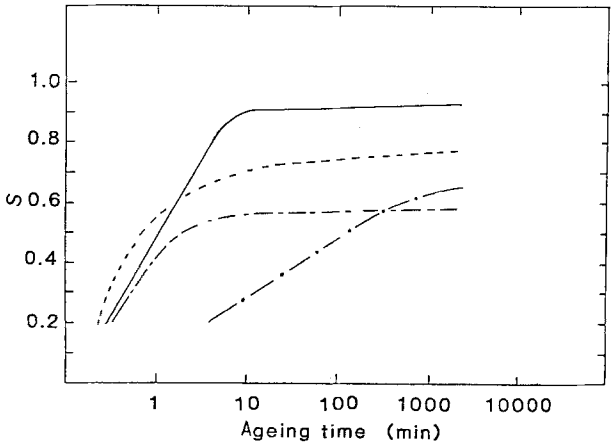

Figure 11 Long-range order parameter (S) as a function of time of heat-treatment at 550 °C for various equiatomic alloys (——) FeCo, (– – –) FeCo–2.45% V and (— — —) FeCo–5.4% V [11], (—·—) FeCo–1% Nb (present work). The data of [11] have been normalized by a factor of 0.8 for comparison with the present results.

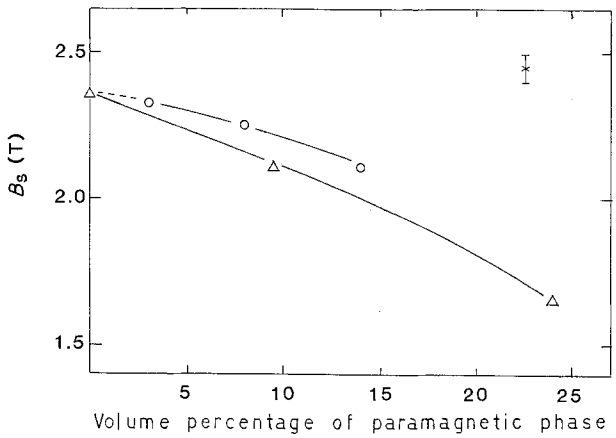

Figure 12 Saturation magnetization (B_s) of furnace-cooled (△) FeCo–V and (○) FeCo–Nb alloys as a function of volume percentage of second phase. The values used for the volume percentage of second phase were determined by Mössbauer spectroscopy [8].

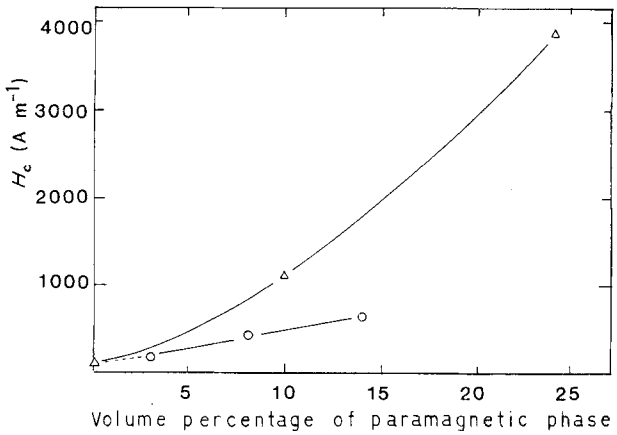

Figure 13 Coercive force (H_c) of furnace-cooled (△) FeCo–V and (○) FeCo–Nb alloys as a function of volume percentage of second phase. The values used for the volume percentage of second phase were determined by Mössbauer spectroscopy [8].

in other FeCo-based systems [1]. The curve for FeCo–Nb lies above that for FeCo–V due to the lower solute content of the ferromagnetic matrix of the former.

The coercive force, H_c, increases with increasing γ_2 content for both alloy systems (Fig. 13). This effect of a dispersion of a paramagnetic second phase is usually attributed to the pinning of ferromagnetic domain walls. The decreasing grain size with increasing volume percentage of the second phase will also contribute to the increment in H_c, as the coercive force of FeCo–2% V has been shown to be inversely proportional to the grain size [1]. The smaller grain size of the FeCo–V alloys may account for the larger H_c values compared to those for the FeCo–Nb alloys.

A specific discussion of the effects on the physical properties of iron–cobalt alloys due to the replacement of vanadium by niobium is presented elsewhere [15].

4.3. Industrial relevance

The marked reduction in the kinetics of ordering and APD growth due to niobium should enable an equiatomic-base alloy to be quenched to the ductile disordered state more readily than is possible with the current vanadium-containing alloys. Indeed, niobium is so effective in slowing down ordering that it may be possible to produce FeCo–Nb alloys containing around 35% Co on an industrial scale; these alloys would be expected to exhibit a higher saturation magnetization, as Fe–35% Co has the highest saturation of any binary alloy. Consistent with this prediction is the observation that the Mössbauer hyperfine field is greater for an Fe–35% Co–0.25% Nb alloy than an Fe–49% Co–0.35% Nb–0.5% Mo alloy [16]. The reduction in the cobalt content would also lead to a saving in raw material costs.

The soft magnetic properties measured in this study are not the optimum for equiatomic FeCo–Nb alloys because of the second phase present. Reducing the niobium content so that all the niobium is in solution will increase B_s and decrease H_c without adversely affecting the kinetics of ordering. The decrease in H_c on reducing the niobium content will be a consequence of removing domain pinning by the second-phase particles, and of an increase in grain size. On the other hand, although the soft magnetic properties are improved by an increase in grain size, d, the reverse is true for ductility of the alloy in the normal service microstructural condition; it has been found that the ductility of ordered equiatomic FeCo-base alloys is proportional to $d^{-1/2}$ [17].

An unfavourable feature of the FeCo–Nb alloys is the low resistivity. This is not important for d.c. applications but could lead to high eddy current losses in a.c. applications.

Acknowledgements

The support of the Brazilian Agencies CAPES and FAPEMIG and of Telcon Metals Ltd is gratefully acknowledged.

References

1. C. M. ORROCK, PhD thesis, London University (1986).
2. R. V. MAJOR and C. M. ORROCK, *IEEE Trans. Mag.* **24** (1988) 1856.
3. S. HALL, private communication (1989).
4. A. W. SMITH and R. D. RAWLINGS, *Phys. Status Solidi (a)* **34** (1976) 117.
5. British Standard BS 5884 (1980).
6. A. E. STEPHENS, H. J. MACKEY and J. R. SYBERT, *J. Appl. Phys.* **42** (1971) 7.
7. A. I. C. PERSIANO and R. D. RAWLINGS, in Proceedings of Conference, "Microstructural characterization of materials by non-microscopic techniques", 5th Riso International Symposium on Metallurgy and Materials Science, edited by N. Hessel Andersen, M. Eldrup, N. Hansen, D. Juml Jansen, T. Leffers, H. Lilholt, O. B. Pedersen and B. N. Singh (Risø National Laboratory, Roskilde, Denmark, 1984) p. 411.
8. *Idem., Phys. Status Solidi (a)* **103** (1987) 547.
9. H. C. FIEDLER and A. M. DAVIS, *Met. Trans.* **1** (1970) 1036.
10. C. D. PITT and R. D. RAWLINGS, *Met. Sci.* **15** (1981) 369.
11. D. W. CLEGG and R. A. BUCKLEY, *ibid.* **7** (1973) 48.
12. J. A. ROGERS, H. M. FLOWER and R. D. RAWLINGS, *ibid.* **9** (1975) 32.
13. P. L. ROSSITER, *J. Phys. F: Metal Phys.* **11** (1981) 615.
14. A. I. C. PERSIANO and R. D. RAWLINGS, to be published.
15. *Idem., ASM J. Mater. Engng* **12** (1990) 21.
16. S. HALL, R. A. MANSUR, H.-D. PFANNES, A. I. C. PERSIANO and R. D. RAWLINGS, in Proceedings of First Latin-American Conference on the Applications of the Mössbauer Effect, Rio de Janeiro, 1988 (World Scientific, London, 1990) p. 263.
17. C. D. PITT and R. D. RAWLINGS, *Met. Sci.* **17** (1983) 261.

Received 30 April
and accepted 19 November 1990